Spectral analysis of stationary random bivariate signals

Julien Flamant, Nicolas Le Bihan, Pierre Chainais

Spectral analysis of stationary random bivariate signals

Julien Flamant, *Student Member, IEEE,* Nicolas Le Bihan, and Pierre Chainais, *Senior Member, IEEE*

***Abstract*—A novel approach towards the spectral analysis of stationary random bivariate signals is proposed. Unlike existing approaches, the proposed framework exhibits a natural link between well-defined statistical objects and physical parameters for bivariate signals. Using the Quaternion Fourier Transform, we introduce a quaternion-valued spectral representation of random bivariate signals seen as complex-valued sequences. This makes possible the definition of a scalar quaternion-valued spectral density and the corresponding autocovariance for bivariate signals. This spectral density can be meaningfully interpreted in terms of frequency-dependent polarization attributes. A natural decomposition of the spectral density of any random bivariate signal in terms of unpolarized and polarized components is introduced. Nonparametric spectral density estimation is investigated, and we introduce the polarization periodogram of a random bivariate signal. Numerical experiments support our theoretical analysis, illustrating the relevance of the approach on synthetic data.**

***Index Terms*—stationary random bivariate signals, polarization, Stokes parameters, degree of polarization**

I. Introduction

RANDOM bivariate signals are 2D vector timeseries. They appear in a large variety of applications, ranging from oceanography [1], [2], to optics [3], radar [4], geophysics [5] or EEG analysis [6] to name but a few. A bivariate signal is usually decomposed in two orthogonal components $u[t]$ and $v[t]$. Thus a bivariate signal $x[t]$ can be either represented as the vector signal $x[t] = (u[t],\, v[t])^T \in \mathbb{R}^2$ or the complex-valued signal $x[t] = u[t] + \boldsymbol{i}v[t]$.

The statistical analysis of signals with vector-valued samples can be carried out using standard multivariate time series analysis techniques (see *e.g* [7, chap. 9] or [8, chap. 11]), bivariate signals are no exception. However, in the signal processing community, bivariate signals have often been described using complex-valued models [9]–[13]. Main advantages are the simplification of algebraic manipulations and geometrical insights offered by the complex representation. To account for the full second-order statistical characterization of the complex signal $x[t] = u[t] + \boldsymbol{i}v[t]$, a usual approach is to define two quantities: the usual autocovariance function and the complementary-covariance function (the relation function in [9]). This leads to the definition of the augmented vector $(x[t], \overline{x[t]})^T \in \mathbb{C}^2$ gathering the signal and its conjugate, and to the related augmented covariance and spectral density matrices [12, chap. 8].

J. Flamant and P. Chainais are with Univ. Lille, CNRS, Centrale Lille, UMR 9189 - CRIStAL - Centre de Recherche en Informatique Signal et Automatique de Lille, 59000 Lille, France. N. Le Bihan is with CNRS/GIPSA-Lab, 11 Rue des mathématiques, Domaine Universitaire, BP 46, 38402 Saint Martin d'Hères cedex, France. Part of this work has been funded by the CNRS, GDR ISIS, within the SUNSTAR interdisciplinary research program.

The *rotary spectrum* analysis [1], [2] is a well-known technique rooted in oceanographic studies. It is based on the decomposition of the spectrum of a complex-valued signal into counter-rotating components. This seminal approach has stimulated many theoretical developments [14]–[19]. The rotary components method is also related to polarization analysis [12], [14]. Both methods provide an equivalent spectral description of the underlying elliptical motion structure of the bivariate signal. The focus on polarization or rotary components usually depends on the field of application: rotary components are more common in oceanography, while optics and radar scientists usually deal with polarization [20]–[24].

In physical sciences, ellipse parameters such as orientation or shape convey fundamental information about the physics that generated the data. An ideal spectral description of bivariate signals should thus provide a natural link between statistical objects and physical parameters.

Existing approaches all rely on the same spectral representation of stationary bivariate processes, which is based on the standard Fourier Transform (FT). For complex signals, it means that negative frequencies must be taken into account, as they provide information about the process. Usually, one considers spectral matrices rather than a scalar spectral density. As a consequence, meaningful physical parameters are not directly "readable" in the state-of-the-art formulations.

We propose a new approach to analyze the spectral content of stationary random bivariate signals. It is based on recent results from [25], [26] and extended to the case of stationary bivariate signals seen as complex-valued signals. This paper provides a well-suited framework for the analysis of stationary bivariate signals which naturally describes the spectral content and the *geometric* or *polarization* content of bivariate signals. Thanks to the definition of the dedicated Quaternion Fourier Transform (QFT), it is possible to describe the spectral content of such signals in terms of polarized and unpolarized parts, which both encode meaningful information about the signal.

This paper structure is as follows. Section II reviews the necessary material regarding quaternions and the QFT. Section III gives the central results of this paper: we introduce the scalar quaternion-valued spectral density of a bivariate signal and its subsequent properties. Results are compared with state-of-the art approaches. In particular the differences between second-order circularity, also called properness, and polarization are stressed. Simple explicit examples are presented in Section IV. Section V deals with nonparametric spectral density estimation, and introduces the polarization periodogram. Our theoretical analysis is supported by numerical experiments in Section VI. Section VII gathers concluding remarks.

II. Quaternion Fourier Transform

A. Quaternion algebra

We review the basic material regarding quaternions and refer to more detailed textbooks (*e.g.* [27]) for a complete overview. Quaternions form a four dimensional noncommutative algebra. Any quaternion $q \in \mathbb{H}$ can be written in its Cartesian form as

$$q = a + b\boldsymbol{i} + c\boldsymbol{j} + d\boldsymbol{k}, \tag{1}$$

where $a, b, c, d \in \mathbb{R}$ and $\boldsymbol{i}, \boldsymbol{j}, \boldsymbol{k}$ are roots of -1 satisfying

$$\boldsymbol{i}^2 = \boldsymbol{j}^2 = \boldsymbol{k}^2 = \boldsymbol{ijk} = -1. \tag{2}$$

The canonical elements $\boldsymbol{i}, \boldsymbol{j}, \boldsymbol{k}$, together with the identity of $\mathbb{H}$ form the quaternion canonical basis given by $\{1, \boldsymbol{i}, \boldsymbol{j}, \boldsymbol{k}\}$. We will use the notation $\mathcal{S}(q) = a \in \mathbb{R}$ to define the *scalar part* of the quaternion q, and $\mathcal{V}(q) = q - \mathcal{S}(q) \in \operatorname{span}\{\boldsymbol{i}, \boldsymbol{j}, \boldsymbol{k}\}$ to denote its *vector part*. We can define the real and imaginary parts of a quaternion q as $\Re(q) = a$, $\Im_{\boldsymbol{i}}(q) = b$, $\Im_{\boldsymbol{j}}(q) = c$, $\Im_{\boldsymbol{k}}(q) = d$. A quaternion is called *pure* if its real (or scalar) part is equal to zero, that is $a = 0$, *e.g.* $\boldsymbol{i}, \boldsymbol{j}, \boldsymbol{k}$ are pure quaternions. The quaternion conjugate of q is $\overline{q} = \mathcal{S}(q) - \mathcal{V}(q)$. The modulus of a quaternion $q \in \mathbb{H}$ is defined by $|q|^2 = q\overline{q} = \overline{q}q = a^2 + b^2 + c^2 + d^2$. The inverse of a non-zero quaternion is defined by $q^{-1} = \overline{q}/|q|^2$. Importantly quaternion multiplication is noncommutative, that is in general for $p, q \in \mathbb{H}$, one has $pq \neq qp$. Involutions with respect to $\boldsymbol{i}, \boldsymbol{j}, \boldsymbol{k}$ are defined as $\overline{q}^{\boldsymbol{i}} = -\boldsymbol{i}q\boldsymbol{i}$, $\overline{q}^{\boldsymbol{j}} = -\boldsymbol{j}q\boldsymbol{j}$, $\overline{q}^{\boldsymbol{k}} = -\boldsymbol{k}q\boldsymbol{k}$. They describe reflections with respect to planes in $\mathbb{R}^4$ and extend somehow the notion of complex conjugation. The combination of quaternion conjugation and involution with respect to an arbitrary pure quaternion $\boldsymbol{\mu}$ is denoted by $q^{\star\boldsymbol{\mu}} := \overline{(\overline{q})}^{\boldsymbol{\mu}} = \overline{(\overline{q}^{\boldsymbol{\mu}})}$ and for instance $(a + b\boldsymbol{i} + c\boldsymbol{j} + d\boldsymbol{k})^{\star\boldsymbol{j}} = a + b\boldsymbol{i} - c\boldsymbol{j} + d\boldsymbol{k}$. For later use, we also introduce the notation $|q|_{\boldsymbol{j}}^2 := qq^{\star\boldsymbol{j}}$.

Quaternions encompass complex numbers. One can construct *complex subfields* of $\mathbb{H}$, *e.g* $\mathbb{C}_{\boldsymbol{j}} = \operatorname{span}\{1, \boldsymbol{j}\}$ or $\mathbb{C}_{\boldsymbol{i}} = \operatorname{span}\{1, \boldsymbol{i}\}$ which are isomorphic to $\mathbb{C}$. Any quaternion can be seen as a pair of complex numbers: let us mention the symplectic decomposition $q = q_1 + \boldsymbol{i}q_2$, $q_1, q_2 \in \mathbb{C}_{\boldsymbol{j}}$, where the quaternion q is splitted into two $\mathbb{C}_{\boldsymbol{j}}$-valued complex numbers. This form is particularly suited for computations performed later on with the quaternion Fourier transform.

Polar forms of quaternions exist. For an arbitrary pure unit quaternion $\boldsymbol{\mu}$ and $\theta \in \mathbb{R}$, we have $\exp(\boldsymbol{\mu}\theta) = \cos\theta + \boldsymbol{\mu}\sin\theta$. It generalizes the notion of complex exponentials and the following polar form was proposed in [28]:

$$q = |q| \exp[\boldsymbol{i}\theta] \exp[-\boldsymbol{k}\chi] \exp[\boldsymbol{j}\varphi], \tag{3}$$

with $(\theta, \chi, \varphi) \in [-\pi/2, \pi/2] \times [-\pi/4, \pi/4] \times [-\pi, \pi]$. This form is particularly useful for quaternion embedding of complex signals, see [25], and in the spectral description of stationary monochromatic signals in Section IV.

B. Quaternion Fourier Transform

We review here briefly the Quaternion Fourier Transform (QFT) introduced in [29] and studied in detail recently in [25]. We refer the reader to these articles for proofs and a detailed presentation. A striking benefit of the QFT is that it provides a well-suited framework for bivariate signals. A key contribution of this paper, the spectral representation Theorem 1 relies on the use of the QFT.

Here we consider only discrete-time (DT) signals: t is a time index such that $x(t\Delta) = x[t]$, where Δ is the sampling step. We assume $\Delta = 1$ in the rest of this paper.

A bivariate signal can be written as a $\mathbb{C}_{\boldsymbol{i}}$-valued signal $x[t] = u[t] + \boldsymbol{i}v[t]$, with u, v real signals. We define its Discrete Time Quaternion Fourier Transform (hereafter denoted QFT) of *axis* $\boldsymbol{j}$ by

$$X(\nu) \triangleq \sum_{t=-\infty}^{+\infty} x[t] \exp(-\boldsymbol{j}2\pi\nu t),\ X(\nu) \in \mathbb{H}. \tag{4}$$

The inverse QFT is given by

$$x[t] = \int_{-1/2}^{+1/2} X(\nu) \exp(\boldsymbol{j}2\pi\nu t) \mathrm{d}\nu. \tag{5}$$

The above relations are directly obtained by discretizing the continuous-time QFT presented in [25], [29] using similar arguments as for the usual FT.

In terms of u, v components, the QFT writes

$$\mathbb{H} \ni X(\nu) = U(\nu) + \boldsymbol{i}V(\nu), \quad U(\nu), V(\nu) \in \mathbb{C}_{\boldsymbol{j}}, \tag{6}$$

where $U(\nu), V(\nu)$ are the standard FTs of u, v: the QFT is performing two standard FT. This may explain why this QFT shares most properties of the classical FT, see [25].

The QFT of $\mathbb{C}_{\boldsymbol{i}}$-valued signals exhibits an $\boldsymbol{i}$-Hermitian symmetry [29]:

$$X(-\nu) = \overline{X(\nu)}^{\boldsymbol{i}}. \tag{7}$$

Eq. (7) shows that, when using the QFT with $x[t] \in \mathbb{C}_{\boldsymbol{i}}$, negative frequencies carry no additional information to positive frequencies about the signal.

The $\boldsymbol{i}$-Hermitian symmetry (7) permits the construction of the *quaternion embedding of a complex signal*, by canceling out negative frequencies of the spectrum. The quaternion embedding of a complex signal is a direct bivariate counterpart of the usual analytic signal and permits to identify both instantaneous phase and polarization (*i.e.* geometric) properties of a complex signal, as discussed in [25].

III. Spectral representation of bivariate stationary random processes

Any bivariate discrete-time random process $x[t]$ can be decomposed as $x[t] = u[t] + \boldsymbol{i}v[t]$, where $u[t], v[t]$ are real-valued discrete-time random processes. The process $x[t]$ is said to be *second-order stationary* if $u[t]$ and $v[t]$ are *jointly second-order stationary*, that is [7, p. 655]:

$$\mathbf{E}\{x[t]\} = \mathbf{E}\{u[t]\} + \boldsymbol{i}\mathbf{E}\{v[t]\} = m \in \mathbb{C}_{\boldsymbol{i}}, \tag{8}$$

$$R_{uu}[t, \tau] = \mathbf{E}\{u[t]u[t-\tau]\} = R_{uu}[\tau],\ R_{uu}[0] < \infty, \tag{9}$$

$$R_{vv}[t, \tau] = \mathbf{E}\{v[t]v[t-\tau]\} = R_{vv}[\tau],\ R_{vv}[0] < \infty, \tag{10}$$

$$R_{uv}[t, \tau] = \mathbf{E}\{u[t]v[t-\tau]\} = R_{uv}[\tau]. \tag{11}$$

Here $\mathbf{E}\{\cdot\}$ denotes the mathematical expectation and R_{uu}, R_{vv} and R_{uv} denote usual autocovariance sequences

(ACVS) and crosscovariance sequences (CCVS) between real-valued sequences. Second-order stationarity ensures that first and second-order moments are finite and do not depend on t; it is simply referred to as *stationarity* in the sequel. All processes are assumed to be zero-mean, *i.e.* $m = 0$, and covariance sequences satisfy sufficient conditions ensuring that their usual Fourier transform exist.

A. Main result

Using the QFT, we derive a spectral representation theorem for any bivariate stationary process $x[t] = u[t] + \boldsymbol{i}v[t]$. The existence of the spectral increments $\mathrm{d}X(\nu)$ follows from the existence of the (usual) spectral increments of $u[t]$ and $v[t]$, see for instance [30, p. 36], [7, p. 246] or [31, p. 344]. Namely, we can write $x[t]$ as the (quaternion) Fourier-Stieltjes integral

$$x[t] = \int_{-1/2}^{+1/2} \mathrm{d}X(\nu) \exp(\boldsymbol{j}2\pi\nu t), \tag{12}$$

where the spectral increments $\mathrm{d}X(\nu) = X(\nu + \mathrm{d}\nu) - X(\nu)$ are quaternion-valued and $X(\nu)$ is an independent additive random measure. The existence roots in two main properties. The QFT restricted to $\mathbb{C}_{\boldsymbol{j}}$-valued processes is isomorphic to the standard FT so that the spectral increments $\mathrm{d}U(\nu), \mathrm{d}V(\nu)$ of $u[t], v[t]$ are $\mathbb{C}_{\boldsymbol{j}}$-valued. Moreover the QFT is left-quaternion-linear, that is $\forall \lambda \in \mathbb{H}$, the QFT of $\lambda x[t]$ is $\lambda X(\nu)$ so that

$$\mathrm{d}X(\nu) = \mathrm{d}U(\nu) + \boldsymbol{i}\mathrm{d}V(\nu). \tag{13}$$

Theorem 1 (Spectral representation of bivariate stationary random processes)**.** *Let $x[t] = u[t] + \boldsymbol{i}v[t]$ be a bivariate stationary process. Suppose that $u[t]$ and $v[t]$ are both harmonizable. Then there exists a quaternion-valued orthogonal process $X(\nu)$ such that*

$$x[t] = \int_{-1/2}^{+1/2} \mathrm{d}X(\nu) \exp(\boldsymbol{j}2\pi\nu t), \tag{14}$$

the integral being defined in the mean-square sense. The process $X(\nu)$ has the following properties:

1) $\forall \nu,\ \mathbf{E}\left\{\mathrm{d}X(\nu)\right\} = 0$,
2) $\forall \nu,\ \mathbf{E}\left\{|\mathrm{d}X(\nu)|^2\right\} + \mathbf{E}\left\{|\mathrm{d}X(\nu)|_{\boldsymbol{j}}^2\right\}\boldsymbol{j} = \Gamma_{xx}(\nu)\mathrm{d}\nu$, *where $\Gamma_{xx}(\nu)$ is the spectral density of x,*
3) *For any $\nu \neq \nu'$, we have*

$$\mathbf{E}\left\{\mathrm{d}X(\nu)\overline{\mathrm{d}X(\nu')}\right\} = \mathbf{E}\left\{\mathrm{d}X(\nu)\mathrm{d}X(\nu')^{\star \boldsymbol{j}}\right\} = 0,$$

which shows that the spectral increments $\mathrm{d}X(\nu)$ are two times orthogonal.

Appendix A proves this theorem that follows the derivation given by Priestley [7], adapted to the QFT setting. Properties 1), 2) and 3) essentially come from the self and joint properties of the spectral increments $\mathrm{d}U(\nu)$ and $\mathrm{d}V(\nu)$. Property 2) introduces the quaternion-valued spectral density of x. This is in fact a *power spectral density* since (see Appendix A) one has

$$\int_{-1/2}^{+1/2} \Gamma_{xx}(\nu)\mathrm{d}\nu = \mathbf{E}\left\{|x[t]|^2\right\} + \mathbf{E}\left\{|x[t]|_{\boldsymbol{j}}^2\right\}\boldsymbol{j} \in \mathbb{H} \tag{15}$$

where the right-hand side contains all the power information of the process $x[t]$.

Note that four (real) power-related quantities are necessary to describe the second-order properties of a bivariate signal, see Section III-C. This argues in favor of the definition of relevant scalar quaternion-valued quantities such as $\Gamma_{xx}(\nu)$.

Note also that our definition of $\Gamma_{xx}(\nu)$ stands in a generalized function sense, allowing to manipulate Dirac distributions.

Since $x[t] = u[t] + \boldsymbol{i}v[t] \in \mathbb{C}_{\boldsymbol{i}}$, the spectral increments additionally satisfy the same $\boldsymbol{i}$-Hermitian symmetry as the QFT of deterministic $\mathbb{C}_{\boldsymbol{i}}$-valued signals, *i.e.*

$$\mathrm{d}X(-\nu) = \overline{\mathrm{d}X(\nu)}^{\boldsymbol{i}}. \tag{16}$$

As a result, the spectral density $\Gamma_{xx}(\nu)$ has symmetry

$$\Gamma_{xx}(-\nu) = \Gamma_{xx}(\nu)^{\star \boldsymbol{i}}. \tag{17}$$

This result shows again that the study of $\mathbb{C}_{\boldsymbol{i}}$-valued (bivariate) signals can be performed using only positive frequencies of its quaternion-valued spectral representation. At each (positive) frequency, a quaternion-valued quantity summarizes both power and polarization properties of x. This will be detailed in Sections III-C and III-D.

Remark. The spectral increments $\mathrm{d}X(\nu)$ are quaternion-valued random variables (RV). It is usual to describe the full second-order statistical structure of a quaternion RV q by the four covariances $\mathbf{E}\{qq^{\star \boldsymbol{\mu}}\}$, $\boldsymbol{\mu} = \boldsymbol{i}, \boldsymbol{j}, \boldsymbol{k}$. These covariances often obey some symmetries characterized by the notion of *properness*. Properness levels of quaternion RV have been investigated by several authors [32]–[34] and reviewed recently in [35]. The spectral increments of a $\mathbb{C}_{\boldsymbol{i}}$-valued process $x[t]$ satisfy the symmetry (16) and thus property 3) of Theorem 1 with $\nu' = -\nu$ yields

$$\mathbf{E}\left\{\mathrm{d}X(\nu)\mathrm{d}X(\nu)^{\star \boldsymbol{i}}\right\} = \mathbf{E}\left\{\mathrm{d}X(\nu)\mathrm{d}X(\nu)^{\star \boldsymbol{k}}\right\} = 0. \tag{18}$$

Eq. (18) shows that the spectral increments $\mathrm{d}X(\nu)$ are $(1, \boldsymbol{j})$-proper in the classification of [35], also denoted as $\mathbb{C}_{\boldsymbol{j}}$-properness in [33]. This can be seen as a generalization of the properness (in the usual complex sense) of the spectral increments of a real stationary process.

B. Covariances, Wiener-Khintchine theorem

Thanks to Theorem 1, we are able to describe the spectral content of random bivariate signals by their spectral density. Usually, this spectral density is introduced by using Wiener-Khintchine theorem once the autocorrelation of the process has been defined. This is not the case here due to the non-commutativity of $\mathbb{H}$: the notion of (auto-)covariance must be carefully defined if one wants to recover a Wiener-Khintchine theorem for quaternion valued processes. To this aim, a natural approach can be to define the autocovariance of x by inverse QFT of $\Gamma_{xx}(\nu)$:

$$\gamma_{xx}[\tau] = \int_{-1/2}^{+1/2} \Gamma_{xx}(\nu) \exp(\boldsymbol{j}2\pi\nu\tau)\mathrm{d}\nu, \tag{19}$$

so that $\gamma_{xx}[\tau]$ is explicitly given by (see Appendix A)

$$\begin{aligned}\gamma_{xx}[\tau] &= R_{uu}[\tau] + R_{vv}[\tau] \\ &\quad + (R_{uu}[\tau] - R_{vv}[\tau])\boldsymbol{j} + 2R_{uv}[\tau]\boldsymbol{k}.\end{aligned} \tag{20}$$

The autocovariance function $\gamma_{xx}[\tau]$ takes its values in $\operatorname{span}\{1, \boldsymbol{j}, \boldsymbol{k}\}$. It is not symmetric in τ, as the term $R_{uv}[\tau]$ is not symmetric in general. More generally one can define the cross-spectral density between two bivariate stationary random processes $x[t] = u_x[t] + \boldsymbol{i}v_x[t]$ and $y[t] = u_y[t] + \boldsymbol{i}v_y[t]$, where $u_k[t], v_k[t] \in \mathbb{R}$, $k = x, y$. Let us denote by $\mathrm{d}X(\nu)$ and $\mathrm{d}Y(\nu)$ their spectral increments. The *cross-spectral density* between x and y is (from adaptation of Eq. (78) in Appendix A)

$$\Gamma_{xy}(\nu)\mathrm{d}\nu = \mathbf{E}\left\{\mathrm{d}X(\nu)\overline{\mathrm{d}Y(\nu)}\right\} + \mathbf{E}\left\{\mathrm{d}X(\nu)\mathrm{d}Y(\nu)^{\star\boldsymbol{j}}\right\}\boldsymbol{j} \tag{21}$$

so that their cross-covariance defined as its inverse QFT reads:

$$\begin{aligned}\gamma_{xy}[\tau] &= R_{u_x u_y}[\tau] + R_{v_y v_x}[\tau] + (R_{u_y v_x}[\tau] - R_{u_x v_y}[\tau])\boldsymbol{i} \\ &\quad + (R_{u_x u_y}[\tau] - R_{v_y v_x}[\tau])\boldsymbol{j} + (R_{u_y v_x}[\tau] + R_{u_x v_y}[\tau])\boldsymbol{k}.\end{aligned} \tag{22}$$

This quaternion-valued cross-covariance encodes the full statistical information about x and y. Eq. (20) and (22) may sound disappointing at first glance, but there is no simple expression of those equations in terms of usual covariance $\mathbf{E}\left\{x[t]\overline{y[t-\tau]}\right\}$ and complementary covariance $\mathbf{E}\left\{x[t]y[t-\tau]\right\}$. However the following Wiener-Khintchine like theorem directly connects $x[t]$ and $y[t]$ to the cross-spectral density (21).

Theorem 2. *Let x and y be two jointly stationary random bivariate signals taking values in $\mathbb{C}_{\boldsymbol{i}}$. Then*

$$\mathbf{E}\left\{\mathrm{d}X(\nu)\overline{\mathrm{d}Y(\nu)}\right\} = \sum_{\tau=-\infty}^{+\infty} \mathbf{E}\left\{x[t]e^{-\boldsymbol{j}2\pi\nu\tau}\overline{y[t-\tau]}\right\} \tag{23}$$

$$\mathbf{E}\left\{\mathrm{d}X(\nu)\mathrm{d}Y(\nu)^{\star\boldsymbol{j}}\right\} = \sum_{\tau=-\infty}^{+\infty} \mathbf{E}\left\{x[t]e^{-\boldsymbol{j}2\pi\nu\tau}y[t-\tau]^{\star\boldsymbol{j}}\right\} \tag{24}$$

where $\mathrm{d}X, \mathrm{d}Y$ are the $\mathbb{H}$-valued spectral increments of x, y of Theorem 1. In the special case $y[t] = x[t]$ one has

$$\mathcal{S}(\Gamma_{xx}(\nu)) = \sum_{\tau=-\infty}^{+\infty} \mathbf{E}\left\{x[t]e^{-\boldsymbol{j}2\pi\nu\tau}\overline{x[t-\tau]}\right\} \tag{25}$$

$$\mathcal{V}(\Gamma_{xx}(\nu)) = \sum_{\tau=-\infty}^{+\infty} \mathbf{E}\left\{x[t]e^{-\boldsymbol{j}2\pi\nu\tau}x[t-\tau]^{\star\boldsymbol{j}}\right\}\boldsymbol{j} \tag{26}$$

Sketch of proof. We start by developing both sides using expressions of $\mathrm{d}X(\nu)$ and $\mathrm{d}Y(\nu)$ in terms of $\mathrm{d}U_k(\nu), \mathrm{d}V_k(\nu)$, $k = x, y$ and $x[t], y[t]$ in terms of $u_k[t], v_k[t]$, $k = x, y$. Then usual rules of quaternion calculus (*e.g.* $\overline{q_1 q_2} = \overline{q_2}\,\overline{q_1}$ for $q_1, q_2 \in \mathbb{H}$; $\boldsymbol{i}q = \overline{q}\boldsymbol{i}$ if $q \in \mathbb{C}_{\boldsymbol{j}}$) permit to simplify both sides. Standard Wiener-Khintchine theorems for real signals lead to the result. □

Let us note finally the following property.

Proposition 1 (Autocorrelation of a sum of independent signals)**.** *If x and y are independent, $\mathbb{C}_{\boldsymbol{i}}$-valued, stationary processes then*

$$\gamma_{x+y,x+y}[\tau] = \gamma_{xx}[\tau] + \gamma_{yy}[\tau] \tag{27}$$

Proof. By direct calculation. □

Proposition 1 is a desirable result, which permits to manipulate quaternion valued autocovariance functions like standard autocovariance functions. Note that this result applies with spectral densities of independent signals x and y as well: the spectral density of $x + y$ is the sum of their spectral densities.

C. Spectral density and Stokes parameters

The spectral density $\Gamma_{xx}(\nu)$ is directly related to Stokes parameters, which are fundamental quantities used to describe the polarization state of electromagnetic waves [36], [37]. Indeed they correspond to physical quantities that are experimentally measurable. Stokes parameters are given by [12], [37]

$$S_0(\nu) = P_{uu}(\nu) + P_{vv}(\nu), \tag{28}$$

$$S_1(\nu) = P_{uu}(\nu) - P_{vv}(\nu), \tag{29}$$

$$S_2(\nu) = 2\Re\left\{P_{uv}(\nu)\right\}, \tag{30}$$

$$S_3(\nu) = 2\Im_{\boldsymbol{j}}\left\{P_{uv}(\nu)\right\}, \tag{31}$$

where we have introduced the usual spectral densities of u and v, P_{uu} and P_{vv}, as well as the usual cross-spectral density P_{uv}.

Theorem 3. *Let $\Gamma_{xx}(\nu)$ be defined by Theorem 1. It can be re-expressed like*

$$\Gamma_{xx}(\nu) = S_0(\nu) + \boldsymbol{i}S_3(\nu) + \boldsymbol{j}S_1(\nu) + \boldsymbol{k}S_2(\nu). \tag{32}$$

where $S_\alpha(\nu)$, $\alpha = 0, 1, 2, 3$ are the Stokes parameters *of x.*

Proof. The two terms appearing in expression 2) of Theorem 1 can be expressed in terms of the spectral increments $\mathrm{d}U(\nu)$ and $\mathrm{d}V(\nu)$ thanks to (13):

$$\begin{aligned}\mathbf{E}\left\{|\mathrm{d}X(\nu)|^2\right\} &= \mathbf{E}\left\{|\mathrm{d}U(\nu)|^2\right\} + \mathbf{E}\left\{|\mathrm{d}V(\nu)|^2\right\} \\ &= (P_{uu}(\nu) + P_{vv}(\nu))\mathrm{d}\nu,\end{aligned} \tag{33}$$

and

$$\begin{aligned}\mathbf{E}\left\{|\mathrm{d}X(\nu)|_{\boldsymbol{j}}^2\right\} &= \mathbf{E}\left\{|\mathrm{d}U(\nu)|^2\right\} - \mathbf{E}\left\{|\mathrm{d}V(\nu)|^2\right\} \\ &\quad + 2\mathbf{E}\left\{\mathrm{d}U(\nu)\overline{\mathrm{d}V(\nu)}\right\}\boldsymbol{i} \\ &= (P_{uu}(\nu) - P_{vv}(\nu) + 2P_{uv}(\nu)\boldsymbol{i})\mathrm{d}\nu.\end{aligned} \tag{34}$$

Then (32) follows from (28) – (31). □

Eq. (32) has a powerful geometric interpretation. Stokes parameters permit to separate the contribution of *polarized* and *unpolarized* components, as discussed next in Section III-E. The scalar part $S_0(\nu)$ of $\Gamma_{xx}(\nu)$ is the total power at frequency ν, *i.e.* the sum of the power of the polarized and unpolarized parts. The vector part describes only the polarized part of x at frequency ν.

D. Poincaré sphere and degree of polarization

Fig. 1 depicts the Poincaré sphere of polarization states [20, p. 125] [37], [38]. At frequency ν, the vector part of $\Gamma_{xx}(\nu)$ – normalized by its scalar part $S_0(\nu)$ – identifies a point on this Poincaré sphere. The angular coordinates $(2\theta, 2\chi)$ are directly related to the *mean ellipse* properties of the signal, *i.e.* θ is the mean orientation and χ is the mean ellipticity.

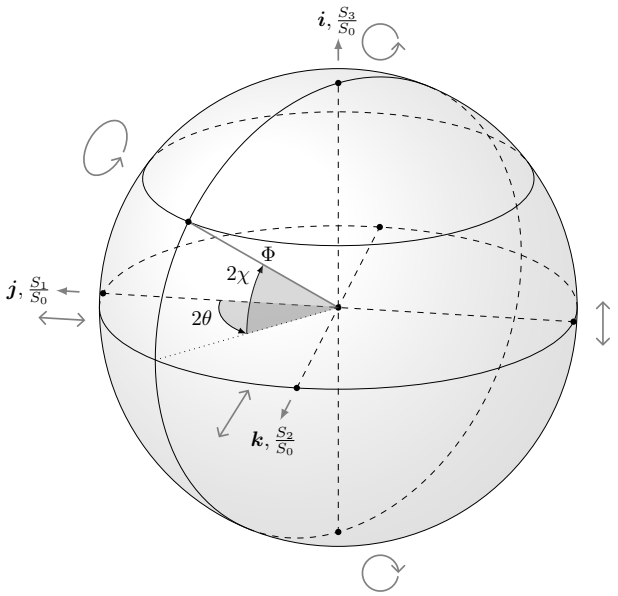

Fig. 1. Poincaré sphere representation of polarization states. Frequency dependence has been dropped for clarity. A point on the sphere corresponds to a particular polarization state, given by its spherical coordinates $(\Phi, 2\theta, 2\chi)$.

At each frequency, the radius of the Poincaré sphere is called the *degree of polarization* $\Phi(\nu)$. Namely,

$$\Phi(\nu) = \frac{\sqrt{S_1^2(\nu) + S_2^2(\nu) + S_3^2(\nu)}}{S_0(\nu)} = \frac{|\mathcal{V}(\Gamma_{xx}(\nu))|}{\mathcal{S}(\Gamma_{xx}(\nu))}, \quad (35)$$

where $\mathcal{V}(\cdot)$ and $\mathcal{S}(\cdot)$ denote the vector and scalar part, respectively. It follows from the definition of $\Phi(\nu)$ that $0 \leq \Phi(\nu) \leq 1$ for all ν. The degree of polarization $\Phi(\nu)$ quantifies the balance between polarized and unpolarized components. This motivates the following vocabulary: the process x is said to be

- fully polarized at frequency ν if $\Phi(\nu) = 1$,
- unpolarized at frequency ν if $\Phi(\nu) = 0$,
- partially polarized at frequency ν if $0 < \Phi(\nu) < 1$.

The degree of polarization is a quantity of fundamental interest in many fields (see *e.g.* [39], [40]). It is invariant to a change of reference frame, making it a robust parameter of interest.

E. Decomposition into polarized and unpolarized parts

The Unpolarized/Polarized part decomposition (hereafter termed UP decomposition) has been evoked in Section III-C. The spectral density of a stationary bivariate signal can be split into two parts: an unpolarized part and a polarized part. Let us rewrite the spectral density of Theorem 1 as

$$\begin{aligned}\Gamma_{xx}(\nu)\mathrm{d}\nu &= [1 - \Phi(\nu)]\, \mathbf{E}\left\{|\mathrm{d}X(\nu)|^2\right\} \\ &\quad + \left[\Phi(\nu)\mathbf{E}\left\{|\mathrm{d}X(\nu)|^2\right\} + \mathbf{E}\left\{|\mathrm{d}X(\nu)|_{\boldsymbol{j}}^2\right\}\boldsymbol{j}\right] \\ &= \Gamma_{xx}^{\mathtt{u}}(\nu)\mathrm{d}\nu + \Gamma_{xx}^{\mathtt{p}}(\nu)\mathrm{d}\nu, \end{aligned} \quad (36)$$

where the u and p superscripts stand for unpolarized and polarized part, respectively. The decomposition (36) is unique. Using Stokes parameters, we get

$$\begin{aligned}\Gamma_{xx}(\nu) &= [1 - \Phi(\nu)]\, S_0(\nu) \\ &\quad + [\Phi(\nu)S_0(\nu) + \boldsymbol{i}S_3(\nu) + \boldsymbol{j}S_1(\nu) + \boldsymbol{k}S_2(\nu)]\end{aligned} \quad (37)$$

which corresponds to the usual decomposition given in standard optics textbooks, see *e.g.* [20, p. 127], [37, p. 551], using quaternions in place of vectors. Eq. (37) highlights how the degree of polarization rules the power repartition between the polarized and unpolarized parts of the spectral density.

F. Comparison with previous work

1) Proper and improper signals: The notion of (im)properness of complex signals, also called second-order circularity, has attracted much interest in the signal processing community over the last two decades, see [9], [12], [13] and references therein. To account for the full second-order statistical structure of a stationary complex signal, one has to consider both the usual autocovariance $R_{xx}[\tau]$ and the complementary covariance $\tilde{R}_{xx}[\tau]$ such that:

$$R_{xx}[\tau] = \mathbf{E}\left\{x[t]\overline{x[t-\tau]}\right\} \quad (38)$$

$$\tilde{R}_{xx}[\tau] = \mathbf{E}\left\{x[t]x[t-\tau]\right\} \quad (39)$$

Proper signals are characterized by a zero complementary covariance sequence, meaning that a signal $x[t]$ is not correlated with its complex conjugate $\overline{x[t-\tau]}$, for all τ. It follows that

$$\forall \tau,\ R_{uu}[\tau] = R_{vv}[\tau] \text{ and } R_{uv}[-\tau] + R_{uv}[\tau] = 0. \quad (40)$$

A direct consequence is that the spectral density (32) of a proper signal $x[t]$ reads

$$\Gamma_{xx}(\nu) = S_0(\nu) + \boldsymbol{i}S_3(\nu) \quad (41)$$

as conditions (40) are equivalent to $S_1(\nu) = S_2(\nu) = 0$ for all ν. Eq. (41) shows that a proper signal is in general partially circularly polarized. This highlights that *polarization* and *properness* of complex random signals are distinct concepts and therefore shall not be confused.

2) Relation to the rotary spectrum approach: To illustrate the relevance of the quaternion-valued spectral density $\Gamma_{xx}(\nu)$ defined in Theorem 1, we compare it to the well-known rotary spectrum approach [1], [2], [15]. This later method decomposes a bivariate signal into a sum of clockwise (CW) and counterclockwise phasors (CCW) – the so-called rotary components [15]. The determination of the rotary components relies on the usual spectral density $P_{xx}(\nu)$ and complementary spectral density $\tilde{P}_{xx}(\nu)$ defined by standard FTs of $R_{xx}[\tau]$ and $\tilde{R}_{xx}[\tau]$, respectively [12].

For $\nu > 0$, the CW rotary power spectrum is given by $P_{xx}(\nu)$, while $P_{xx}(-\nu)$ gives the CCW rotary power spectrum. The rotary coherence (*i.e.* correlation between CW and CCW components) is controlled by $\tilde{P}_{xx}(\nu)$, which is in general complex-valued.

The rotary spectra can be expressed in terms of Stokes parameters like [12, p. 213]

$$P_{xx}(\nu) = S_0(\nu) + S_3(\nu), \quad \tilde{P}_{xx}(\nu) = S_1(\nu) + \boldsymbol{i}S_2(\nu). \quad (42)$$

Since $S_0(\nu)$ is even and $S_3(\nu)$ is odd, $P_{xx}(\nu)$ shows no particular symmetry. Moreover, we see that $P_{xx}(\nu)$ combines in one real scalar two very different quantities: $S_0(\nu)$ is related to the total power, and $S_3(\nu)$ gives the (signed) power of the circularly polarized part. This is not surprising since the pair $(P_{xx}(\nu), \tilde{P}_{xx}(\nu))$ was introduced to account for improperness properties of complex-valued signals, not polarization properties. In contrast, $\Gamma_{xx}(\nu)$ naturally separates the total power from the polarization information.

The rotary spectrum and the quaternion-valued approach provide equivalent representations. However, the quaternion-valued spectral density Γ_{xx} provides a direct interpretation of physical quantities, the Stokes parameters. These parameters appear naturally in the components of Γ_{xx}. The use of the QFT to study bivariate signals provides a well-suited framework for a meaningful and rooted in physics "geometric spectral analysis". This approach demonstrates that the use of higher dimensional algebra in the definition of the FT permits a direct connection between well-defined mathematical objects and relevant physical quantities without introducing any *a priori* structural model, *e.g.* as in [12], [15].

IV. Examples

A. Bivariate monochromatic signals

Let the bivariate monochromatic signal $x[t]$ be defined by

$$\begin{aligned} x[t] = 2ae^{\boldsymbol{i}\theta}(&\cos\chi\cos[2\pi\nu_0 t + \varphi] \\ &+\boldsymbol{i}\sin\chi\sin[2\pi\nu_0 t + \varphi]), \end{aligned} \tag{43}$$

where a, χ, θ are the parameters of the elliptical polarization and φ is a random phase term uniformly distributed on $[0, 2\pi)$. The autocovariance of $x[t]$ (see (20)) now reads:

$$\begin{aligned} \gamma_{xx}[\tau] = &2S_0\cos[2\pi\nu_0\tau] + \boldsymbol{j}2S_1\cos[2\pi\nu_0\tau] \\ &+ 2\boldsymbol{k}\left(S_2\cos[2\pi\nu_0\tau] + S_3\sin[2\pi\nu_0\tau]\right). \end{aligned} \tag{44}$$

where $S_0 = a^2$, $S_1 = a^2\cos(2\theta)\cos(2\chi)$, $S_2 = a^2\sin(2\theta)\cos(2\chi)$ and $S_3 = a^2\sin(2\chi)$ are the Stokes parameters. The autocovariance is not symmetric. The value of S_3 controls the odd contribution, whereas the remaining terms are all even. It therefore follows that the autocovariance function of a monochromatic signal is even if and only if the signal is linearly polarized, *i.e.* $S_3 = 0$. The spectral density $\Gamma_{xx}(\nu)$ is obtained by the QFT of $\gamma_{xx}[\tau]$ given in (44):

$$\Gamma_{xx}(\nu) = \Gamma_{xx}^{\nu_0}\delta(\nu - \nu_0) + \Gamma_{xx}^{\nu_0\star\boldsymbol{i}}\delta(\nu + \nu_0), \tag{45}$$

where $\Gamma_{xx}^{\nu_0} = S_0 + \boldsymbol{i}S_3 + \boldsymbol{j}S_1 + \boldsymbol{k}S_2$. From Stokes parameters above, the degree of polarization is at frequency ν_0

$$\Phi(\nu_0) = \frac{|\mathcal{V}(\Gamma_{xx}(\nu_0))|}{\mathcal{S}(\Gamma_{xx}(\nu_0))} = \frac{\sqrt{S_1^2 + S_2^2 + S_3^2}}{S_0} = 1 \tag{46}$$

which highlights the fact that *a bivariate monochromatic signal is always fully polarized*.

B. Bivariate white noise

Consider the process $w[t] = u[t] + \boldsymbol{i}v[t]$ where u, v are both real, i.i.d. and jointly second-order stationary with properties:

$$\begin{aligned} &\mathbf{E}\{u\} = \mathbf{E}\{v\} = 0, \\ &\mathbf{E}\{u^2\} = \sigma_u^2,\ \mathbf{E}\{v^2\} = \sigma_v^2,\ \mathbf{E}\{uv\} = \rho_{uv}\sigma_u\sigma_v. \end{aligned} \tag{47}$$

Since u, v are i.i.d., the corresponding covariances are

$$R_{uu}[\tau] = \sigma_u^2\delta_{\tau,0},\ R_{vv}[\tau] = \sigma_v^2\delta_{\tau,0},\ R_{uv}[\tau] = \rho_{uv}\sigma_u\sigma_v\delta_{\tau,0}. \tag{48}$$

which yields the autocorrelation of w using (20)

$$\gamma_{ww}[\tau] = \left[\sigma_u^2 + \sigma_v^2 + \boldsymbol{j}(\sigma_u^2 - \sigma_v^2) + 2\boldsymbol{k}\rho_{uv}\sigma_u\sigma_v\right]\delta_{\tau,0}. \tag{49}$$

The spectral density is obtained by QFT:

$$\Gamma_{ww}(\nu) = \sigma_u^2 + \sigma_v^2 + \boldsymbol{j}(\sigma_u^2 - \sigma_v^2) + 2\boldsymbol{k}\rho_{uv}\sigma_u\sigma_v. \tag{50}$$

This spectral density is constant. It has no $\boldsymbol{i}$-component, so that $S_3(\nu) = 0$ for all ν. As a consequence, an *arbitrary second-order stationary bivariate or complex white noise shows no ellipticity. It is always either unpolarized, or linearly polarized (fully or partially). The polarization properties are identical at all frequencies*.

The polarization degree defined by (35) is:

$$\Phi = \frac{\sqrt{(\sigma_u^2 - \sigma_v^2)^2 + 4\rho_{uv}^2\sigma_u^2\sigma_v^2}}{\sigma_u^2 + \sigma_v^2}, \tag{51}$$

where we see that $x[t]$ is unpolarized at all frequencies iff $\sigma_u = \sigma_v$ and $\rho_{uv} = 0$. This case is equivalent to proper white noise. When $\Phi \neq 0$, the angle θ of the linear polarization is given by $\theta = 0$ if $\rho_{uv} = 0$ and by

$$\begin{cases} \theta &= \frac{1}{2}\mathrm{atan2}\left[\frac{2\rho_{uv}\sigma_u\sigma_v}{(\sigma_u^2 - \sigma_v^2)}\right],\ \text{if } \sigma_u \neq \sigma_v \\ \theta &= \pi/4, \text{if } \sigma_u = \sigma_v \end{cases} \tag{52}$$

when $\rho_{uv} \neq 0$ and where atan2 denotes the four-quadrant inverse tangent.

The UP decomposition of bivariate white noise gives a simple procedure to simulate bivariate white noise with desired polarization properties. Let $0 \leq \Phi \leq 1$ be the desired degree of polarization, $\theta \in [-\pi/2, \pi/2]$ the orientation angle and $S_0 > 0$ the total intensity. Let $w^{\mathrm{u}}[t]$ be an unpolarized white noise, $\mathbb{C}_{\boldsymbol{i}}$-valued, such that $R_{w^{\mathrm{u}}w^{\mathrm{u}}}[\tau] = \delta_{\tau,0}$. Let $w^{\mathrm{p}}[t]$ be a real-valued white noise sequence of unit variance. Assume further that $w^{\mathrm{u}}[t]$ and $w^{\mathrm{p}}[t]$ are independent. Then the white noise $w[t]$ constructed as

$$w[t] = \sqrt{1 - \Phi}\sqrt{S_0}w^{\mathrm{u}}[t] + \sqrt{\Phi}\sqrt{S_0}\exp(\boldsymbol{i}\theta)w^{\mathrm{p}}[t] \tag{53}$$

has spectral density $\Gamma_{ww}(\nu) = S_0 + \boldsymbol{j}\Phi S_0\cos 2\theta + \boldsymbol{k}\Phi S_0\sin 2\theta$ where one recognizes a linear polarization state with spherical coordinates $(\Phi, 2\theta, 0)$, see Fig. 1.

C. Bivariate monochromatic signal in white noise

Consider the signal $y[t] = x[t] + w[t]$, where $x[t]$ is a bivariate monochromatic signal and $w[t]$ is a bivariate white noise. Assume moreover that $x[t]$ and $w[t]$ are independent.

From Proposition 1 the spectral density of y is directly given by the sum of their spectral densities:

$$\Gamma_{yy}(\nu) = \Gamma_{xx}^{\nu_0}\delta(\nu-\nu_0) + \Gamma_{xx}^{\nu_0\star\boldsymbol{i}}\delta(\nu+\nu_0) + \Gamma_{ww}(\nu) \quad (54)$$

where $\Gamma_{ww}(\nu)$ is given by (50) and $\Gamma_{xx}^{\nu_0} = S_{0,x} + \boldsymbol{i}S_{3,x} + \boldsymbol{j}S_{1,x} + \boldsymbol{k}S_{2,x}$; the $S_{\alpha,x}$ denote the Stokes parameters of x. At $\nu=\nu_0$ the spectral density writes $\Gamma_{yy}^{\nu_0} = S_{0,y} + \boldsymbol{i}S_{3,y} + \boldsymbol{j}S_{1,y} + \boldsymbol{k}S_{2,y}$ where

$$\begin{aligned} &S_{0,y} = S_{0,x} + \sigma_u^2 + \sigma_v^2, \quad S_{1,y} = S_{1,x} + \sigma_u^2 - \sigma_v^2 \\ &S_{2,y} = S_{2,x} + 2\rho_{uv}\sigma_u\sigma_v, \quad S_{3,y} = S_{3,x}. \end{aligned} \quad (55)$$

First, we see that $S_{1,y}$ and $S_{2,y}$ parameters are mixing polarization properties of x and w. Since $S_{3,y}$ is not modified in presence of white noise, only the direction of polarization changes, not the ellipticity. The output degree of polarization (at $\nu=\nu_0$) takes a simple form when the noise is unpolarized since $\sigma_u = \sigma_v$ and $\rho_{uv}=0$ in this case:

$$\Phi_y = \frac{\sqrt{S_{1,x}^2 + S_{2,x}^2 + S_{3,x}^2}}{S_{0,x} + \sigma_u^2 + \sigma_v^2} = \frac{\mathrm{SNR}}{\mathrm{SNR}+1}\Phi_x \leq \Phi_x \quad (56)$$

where $\mathrm{SNR} = S_{0,x}/(\sigma_u^2+\sigma_v^2)$ is the signal-to-noise ratio (SNR). The degree of polarization decreases with the SNR.

V. Spectral density estimation

We propose two nonparametric spectral density estimation methods, and derive their properties. In particular, we investigate the problem of estimating the degree of polarization. In the remainder of this paper, we consider a bivariate stationary signal $x[t] = u[t] + \boldsymbol{i}v[t]$ consisting of N samples such that $t = 0, 1, \ldots N-1$ and with sampling size $\Delta = 1$.

A. A naive spectral estimator: the polarization periodogram

The first basic spectral density estimator is the *polarization periodogram* $\hat{\Gamma}_{xx}^{(p)}(\nu)$. The underlying rationale is very close to the derivation of the usual periodogram. One starts by computing an estimator $\hat{\gamma}_{xx}^{(p)}[\tau]$ of the autocovariance sequence $\gamma_{xx}[\tau]$. It is done by combining usual (biased) estimators of auto- and cross-covariance sequences, *e.g.*:

$$\hat{R}_{uv}^{(p)}[\tau] = \frac{1}{N}\sum_{t=1}^{N-\tau} u[t+\tau]v[t],\ \tau = 0, 1, \ldots N-1 \quad (57)$$

where $\hat{R}_{uv}^{(p)}[\tau] = \hat{R}_{vu}^{(p)}[-\tau]$ for $\tau = -1, \ldots, -(N-1)$ and $\hat{R}_{uv}^{(p)}[\tau] = 0$ for $|\tau| \geq N$. Auto-covariance estimators follow from (57). Then taking the QFT of $\hat{\gamma}_{xx}^{(p)}[\tau]$ given by (20) yields the *polarization periodogram*, which reads (after simplification)

$$\begin{aligned} \hat{\Gamma}_{xx}^{(p)}(\nu) = N^{-1}&\left|\sum_{t=1}^{N} x[t]e^{-\boldsymbol{j}2\pi\nu t}\right|^2 \\ &+ N^{-1}\left|\sum_{t=1}^{N} x[t]e^{-\boldsymbol{j}2\pi\nu t}\right|^2_{\boldsymbol{j}} \end{aligned} \quad (58)$$

Alike the classical periodogram, this estimator is a biased, inconsistent estimator of the spectral density $\Gamma_{xx}(\nu)$. One has

$$\mathbf{E}\left\{\hat{\Gamma}_{xx}^{(p)}(\nu)\right\} = \int_{-1/2}^{+1/2} \mathcal{F}_N(\nu-\nu')\Gamma_{xx}(\nu')\mathrm{d}\nu' \quad (59)$$

where $\mathcal{F}_N(\nu) = \sin^2(\pi N\nu)/[N\sin^2(\pi\nu)]$ is the Fejér kernel. It follows that the polarization periodogram is only asymptotically unbiased. Note however that in the case of white noise, as $\Gamma_{ww}(\nu)$ is constant, the polarization periodogram is unbiased for any N. This is a bivariate counterpart of a classical result, see *e.g.* [41, p. 202].

Alike in standard spectral analysis [41], data tapers are to be employed to produce a direct spectral estimator with better bias properties than the naive polarization periodogram.

B. Multitapering

The multitaper method is a well established technique [41]–[43] which produces a spectral density estimate with reduced variance, while maintaining good bias properties. The basic idea is to compute a series of K *direct estimators* $\hat{\Gamma}_{xx}^{k}(\nu)$, $k = 0, 1, \ldots K-1$ that are approximately uncorrelated [41]. The k-th spectral estimator reads

$$\begin{aligned} \hat{\Gamma}_{xx}^{k}(\nu) = &\left|\sum_{t=1}^{N} h_k[t]x[t]e^{-\boldsymbol{j}2\pi\nu t}\right|^2 \\ &+ \left|\sum_{t=1}^{N} h_k[t]x[t]e^{-\boldsymbol{j}2\pi\nu t}\right|^2_{\boldsymbol{j}}, \end{aligned} \quad (60)$$

where the h_k's are real-valued sequences of size N. They are normalized ($\sum_{t=0}^{N-1} h_k[t]^2 = 1$) and orthogonal

$$\sum_{t=0}^{N-1} h_k[t]h_{k'}[t] = \delta_{k,k'}. \quad (61)$$

Functions satisfying these conditions together with good leakage properties are for instance the Slepian tapers [44]. Then the multitaper estimate is obtained by averaging:

$$\hat{\Gamma}_{xx}^{(\mathrm{mt})}(\nu) = \frac{1}{K}\sum_{k=1}^{K}\hat{\Gamma}_{xx}^{k}(\nu). \quad (62)$$

Regarding the choice of K [43], let denote the signal duration by $T = N\Delta$ (here $\Delta=1$) and the desired bandwidth by $2B = 2W/(N\Delta)$, where $W \in \mathbb{N}^*$. $2W$ corresponds to the number of frequency samples over which the spectral estimate is smoothed out by multitapering. The number of Slepian tapers is $K = 2TB - 1 = 2W - 1$ which does not depend on N. Moreover a good bias-variance tradeoff is guaranteed for small values of W, typically $W \leq 5$ so that $K \leq 10$.

C. Estimation of the degree of polarization

1) Theoretical properties: The estimation of the degree of polarization (35) has attracted interest in the signal processing community [45], [46] in relation to many fields [39], [40].

A naive estimator (at frequencies where the polarization periodogram is nonzero) based on the polarization periodogram would be trivial since:

$$\hat{\Phi}^{(p)}(\nu) = \frac{|\mathcal{V}(\hat{\Gamma}_{xx}^{(p)}(\nu))|}{\mathcal{S}(\hat{\Gamma}_{xx}^{(p)}(\nu))} = 1, \tag{63}$$

which is systematically biased, except for frequencies where $x[t]$ is fully polarized. In a situation where M approximately uncorrelated estimates of the spectral density are available (having multiple realizations of x or using a multitaper estimate (62), in which case $M = K$) one can form a new estimate of the degree of polarization as

$$\hat{\Phi}^{M}(\nu) = \frac{|\sum_{m=1}^{M} \mathcal{V}(\hat{\Gamma}_{xx}^{m}(\nu))|}{\sum_{m=1}^{M} \mathcal{S}(\hat{\Gamma}_{xx}^{m}(\nu))}, \tag{64}$$

which is a better estimator of Φ than (63). Medkour and Walden[1] [45] studied theoretically this estimator in a Gaussian setting and showed that it is unbiased in the limit $M \to \infty$.

2) Numerical study: We propose to numerically study the performances of the estimator (64). To avoid spectral blurring effects, we consider the (Gaussian) white noise case since in that case the polarization periodogram is an unbiased estimator of the spectral density:

$$\mathbf{E}\left\{\hat{\Gamma}_{ww}^{(p)}(\nu)\right\} = \Gamma_{ww}(\nu). \tag{65}$$

The spectral density $\Gamma_{ww}(\nu)$ is given by (50) and is constant. The UP decomposition (53) of bivariate white noise permits to generate white noise with prescribed polarization properties. We fix $S_0 = 1, \theta = 0$ without loss of generality. We generate M independent bivariate white Gaussian noise sequences of length $N = 10^5$ samples for several values of Φ. This leads to M independent periodogram estimates of the spectral density (58). The degree of polarization is then estimated by averaging in (64) for each positive Fourier frequency $\nu_k = k/N$, $0 \leq k \leq N/2$. These $N/2$ degree of polarization estimates are independent[2]. Since bivariate white noise has a constant spectral density, they can thus be averaged out to compute an estimate of $\mathbf{E}\left\{\hat{\Phi}^{M}\right\}$.

Fig. 2 depicts the bias in the estimation of the degree of polarization, for $M = 1, 2, 5, 10, 20, 50$ and 500. Given M, the bias increases as the true degree of polarization goes to 0. The bias decreases with larger values of M, and becomes negligible for $M \to \infty$. Note that for typical values of M (2 to 10) used in multitaper estimation, the bias remains significant up to $\Phi \simeq 0.6$. Our results agree with those of [45].

It is worth noting that spectra of polarization attributes can be more difficult to obtain than simple power spectra, as the observation of many realizations may be required to reach a good accuracy.

[1]Their approach is based on spectral matrices rather than the quaternion-valued spectral density introduced here. However this does not change the nature of their results, since definitions of the degree of polarization are identical.

[2]More precisely, recall that for a white Gaussian noise the $N/2$ samples corresponding to the positive Fourier frequencies $\nu_k = k/N$, $0 \leq k \leq N/2$ are independent [41, p.222]. The same result holds here for the QFT and the bivariate white noise.

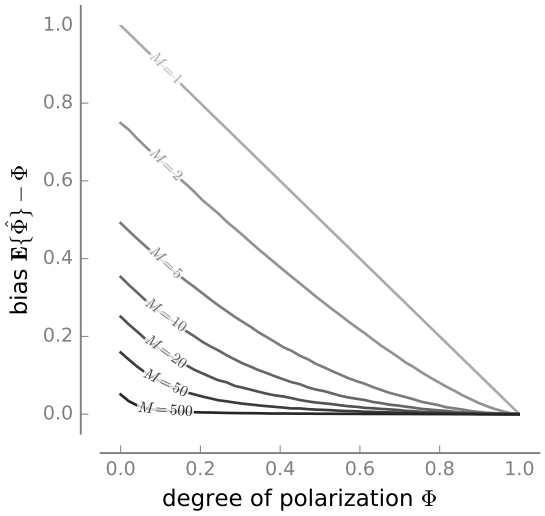

Fig. 2. Estimation bias of the degree of polarization obtained by averaging M independent polarization periodogram estimates. The bias is smaller for large values of M and a degree of polarization close to unity.

VI. Numerical validation

We consider the synthetic bivariate signal of Section IV-C $y[t] = x[t] + w[t]$, where x is a bivariate monochromatic signal defined by (43) and where w is a bivariate white Gaussian noise given in (53). All signals are of length $N = 1024$. We consider positive frequencies only, as negative frequencies can be obtained by symmetry (17).

The frequency of the monochromatic signal x is set to $\nu_0 = 128/N = 0.125$. At frequency ν_0, the signal x has Stokes parameters: $S_{0,x}(\nu_0) = 1$, $s_{1,x}(\nu_0) = S_{1,x}(\nu_0)/S_{0,x}(\nu_0) = -0.354$, $s_{2,x}(\nu_0) = S_{2,x}(\nu_0)/S_{0,x}(\nu_0) = -0.612$, $s_{3,x}(\nu_0) = S_{3,x}(\nu_0)/S_{0,x}(\nu_0) = 0.707$ and $\Phi_x(\nu_0) = 1$ since x is monochromatic. For $\nu \neq \nu_0$, all Stokes parameters $S_{\alpha,x}$, $\alpha = 0, ..., 3$ are zero. Equivalently, x is defined by $a_x = 1$, $\theta_x = -\pi/3$ and $\chi_x = \pi/8$ using Eq. (43).

The white noise signal w has constant-frequency Stokes parameters (see Section IV-B) such that $S_{0,w}(\nu) = 10^{-2}$, $\Phi_w(\nu) = 0.2$, $\theta_w(\nu) = \pi/8$ or equivalently, $s_{1,w}(\nu) = 0.141$ and $s_{2,w}(\nu) = 0.141$. Since w is a white noise sequence (and thus has no memory), $s_{3,w}(\nu) = 0$ for any ν.

The spectral description of $y[t] = x[t] + w[t]$ was derived explicitly in Section IV-C. Using expressions (54) and (55) we see that the resulting Stokes parameters at $\nu \neq \nu_0$ are those of w. At frequency ν_0 we have

$$\begin{aligned} &S_{0,y}(\nu_0) = S_{0,x}(\nu_0) + S_{0,w}(\nu_0), \\ &S_{1,y}(\nu_0) = S_{1,x}(\nu_0) + S_{1,w}(\nu_0), \\ &S_{2,y}(\nu_0) = S_{2,x}(\nu_0) + S_{2,w}(\nu_0), \quad S_{3,y}(\nu_0) = S_{3,x}(\nu_0). \end{aligned} \tag{66}$$

For frequency ν_0, the normalized Stokes parameters and polarization degree are

$$\begin{aligned} s_{1,y}(\nu_0) = -0.349,\ s_{2,y}(\nu_0) = -0.605, \\ s_{3,y}(\nu_0) = 0.700,\ \Phi_y(\nu_0) = 0.989. \end{aligned} \tag{67}$$

Due to the polarization properties of w, the polarization properties at ν_0 of y are not the same as those of x.

To investigate the estimation of the spectral density of y, we have generated $M = 20$ realizations. For each realization, we compute the polarization periodogram and the multitaper estimate using $K = 5$ Slepian tapers corresponding to a bandwidth-duration product $2TB = 6$. To reduce the bias of the degree of polarization estimate, those estimates are averaged to produce a polarization periodogram estimate and a multitaper estimate. This also reduces bias on normalized Stokes parameters estimates, as one expects the estimates of s_1, s_2, s_3 to be biased as they depend on the value of the degree of polarization.

Fig. 3 shows one realization of the process y and subsequent simulation results. As expected the (averaged) multitaper estimate has less variance and leakage bias than the (averaged) polarization periodogram. Theoretical values of the components of the spectral density are indicated by arrows on the right for noise level and horizontal thin lines at ν_0. One first observes that the periodogram yields a better estimate of $S_0(\nu_0)$, which can be explained by the smoothing effect of multitapering. However, multitapering yields a better bias-variance tradeoff on estimates of all relative quantities such as $s_\alpha(\nu)$ and $\Phi(\nu)$. In particular note that the standard deviation of the estimate of $s_1(\nu)$ from the periodogram is of the order of magnitude of $s_1(\nu_0)$. This corresponds to the expected behaviour of these estimators.

VII. Conclusion

This paper provides a powerful and relevant framework for an interpretable and efficient spectral analysis of stationary bivariate processes. The richness of the quaternion algebra permits a fruitful interplay between mathematical tools and physical features. Using the QFT, we have introduced the quaternion-valued spectral representation of a bivariate stationary random signal. As a result, the quaternion-valued spectral density is defined. Moreover it can be expressed in terms of Stokes parameters. It permits a direct physical interpretation of both power and polarization features of the signal. By introducing the degree of polarization, the spectral density can be written as the sum of unpolarized and polarized components. Simple examples demonstrate the relevance of the approach. Usual tools of standard spectral analysis can be adapted to the nonparametric spectral density estimation of bivariate signals. We emphasize the issue raised by the estimation of the degree of polarization and of polarization attributes. These key quantities are relevant to the analysis of bivariate signals but require special care. Our approach is very generic and easy to use thanks to the companion `BiSPy` package[3]. It generalizes the standard toolbox of spectral analysis to bivariate stationary signals and paves the way to new developments in the simulation, estimation and filtering of bivariate signals.

Appendix A
Proof of the spectral representation Theorem 1

The proof is divided in two parts, for clarity.

[3]https://github.com/jflamant/bispy

a) Existence: Let $x[t] = u[t] + \boldsymbol{i}v[t]$, where $u[t], v[t]$ are real-valued, zero-mean, harmonizable stationary processes. These real processes admit a spectral representation, such that

$$\begin{aligned} u[t] &= \int_{-1/2}^{+1/2} \mathrm{d}U(\nu) \exp(\boldsymbol{j}2\pi\nu t), \\ v[t] &= \int_{-1/2}^{+1/2} \mathrm{d}V(\nu) \exp(\boldsymbol{j}2\pi\nu t), \end{aligned} \tag{68}$$

where $\mathrm{d}U, \mathrm{d}V$ are the $\mathbb{C}_{\boldsymbol{j}}$-valued spectral increments of u, v respectively. Recall that the QFT applied to $\mathbb{C}_{\boldsymbol{j}}$-valued signals is equivalent to the usual Fourier transform. By linearity of the QFT, the spectral increments of x are $\mathrm{d}X(\nu) = \mathrm{d}U(\nu) + \boldsymbol{i}\mathrm{d}V(\nu)$, so that

$$x[t] = \int_{-1/2}^{+1/2} \mathrm{d}X(\nu) \exp(\boldsymbol{j}2\pi\nu t) \tag{69}$$

holds for all t in the mean-square sense.

b) Properties of the spectral increments: The properties of the spectral increments $dX(\nu)$ are a direct consequence of the properties of the spectral increments of u and v, respectively. If x is assumed zero-mean stationary,

$$\begin{aligned} \forall t, \mathbf{E}\left\{x[t]\right\} = \int_{-1/2}^{+1/2} \mathbf{E}\left\{\mathrm{d}X(\nu)\right\} \exp(\boldsymbol{j}2\pi\nu t) = 0 \\ \Rightarrow \mathbf{E}\left\{\mathrm{d}X(\nu)\right\} = \mathbf{E}\left\{x[t]\right\} = 0. \end{aligned} \tag{70}$$

Turning to the second-order properties of the spectral increments, let us consider the spectral representation of u and v. Second-order stationarity implies that (see [7] for details)

$$\forall \nu \neq \nu', \begin{cases} \mathbf{E}\left\{\mathrm{d}U(\nu)\overline{\mathrm{d}U(\nu')}\right\} &= 0 \\ \mathbf{E}\left\{\mathrm{d}V(\nu)\overline{\mathrm{d}V(\nu')}\right\} &= 0 \end{cases} \tag{71}$$

and autocorrelation functions of u, v read

$$\mathbf{E}\left\{u[t]u[t-\tau]\right\} = \int_{-1/2}^{+1/2} \mathbf{E}\left\{|\mathrm{d}U(\nu)|^2\right\} e^{\boldsymbol{j}2\pi\nu\tau}, \tag{72}$$

$$\mathbf{E}\left\{v[t]v[t-\tau]\right\} = \int_{-1/2}^{+1/2} \mathbf{E}\left\{|\mathrm{d}V(\nu)|^2\right\} e^{\boldsymbol{j}2\pi\nu\tau}. \tag{73}$$

The quantity $\mathbf{E}\left\{|\mathrm{d}U(\nu)|^2\right\}$ is interpreted as the spectral density P_{uu} of u times $\mathrm{d}\nu$. The same result holds for v.

To fully characterize the spectral increments of x, we also need the covariance between the spectral increments of u and v. Since u and v are jointly second-order stationary,

$$\forall \nu \neq \nu', \mathbf{E}\left\{\mathrm{d}U(\nu)\overline{\mathrm{d}V(\nu')}\right\} = 0, \tag{74}$$

and the cross-correlation function reads

$$\mathbf{E}\left\{u[t]v[t-\tau]\right\} = \int_{-1/2}^{+1/2} \mathbf{E}\left\{\mathrm{d}U(\nu)\overline{\mathrm{d}V(\nu)}\right\} e^{\boldsymbol{j}2\pi\nu\tau}. \tag{75}$$

As a result we have from (71) and (74):

$$\forall \nu \neq \nu', \mathbf{E}\left\{\mathrm{d}X(\nu)\overline{\mathrm{d}X(\nu')}\right\} = 0, \tag{76}$$

$$\forall \nu \neq \nu', \mathbf{E}\left\{\mathrm{d}X(\nu)\mathrm{d}X(\nu')^{\star\boldsymbol{j}}\right\} = 0. \tag{77}$$

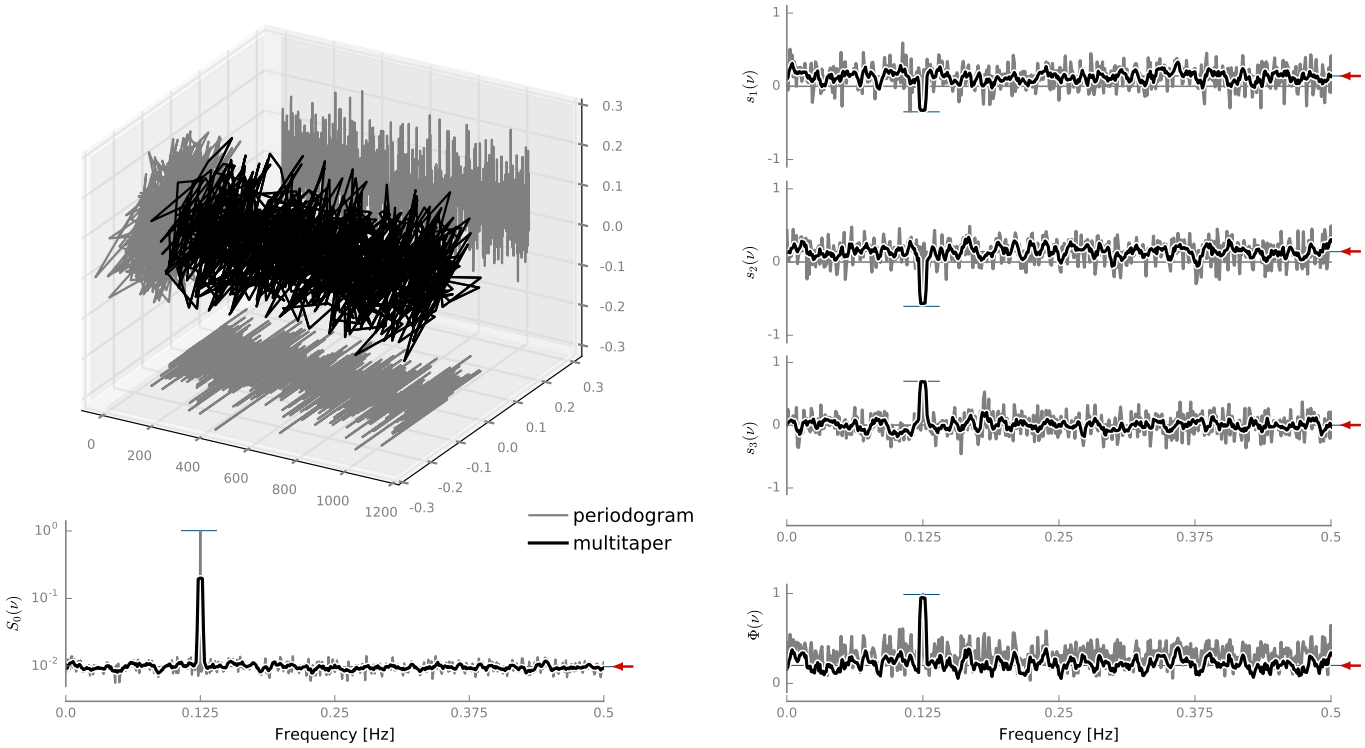

Fig. 3. Spectral density estimation of the $y = x + w$ signal, where x is a monochromatic bivariate signal and w is a bivariate white Gaussian noise. Two estimates are presented, the averaged polarization periodogram and averaged multitaper estimate (computed with $K = 5$ Slepian tapers). They are constructed by averaging single estimates obtained via $M = 20$ independent observations of the process y. Thin lines and arrows indicate the theoretical values of intensity parameter $S_0(\nu)$, normalized Stokes parameters $s_\alpha(\nu) = S_\alpha(\nu)/S_0(\nu)$, $\alpha = 1, 2, 3$ and degree of polarization $\Phi(\nu)$.

When $\nu' = \nu$, the properties are summarized by the spectral density $\Gamma_{xx}(\nu)$

$$\mathbf{E}\left\{|\mathrm{d}X(\nu)|^2\right\} + \mathbf{E}\left\{\mathrm{d}X(\nu)\mathrm{d}X(\nu)^{\star \boldsymbol{j}}\right\}\boldsymbol{j} = \Gamma_{xx}(\nu)\mathrm{d}\nu \quad (78)$$

which separates in quaternion algebra the information contained in the two moments of the spectral increments. This theorem holds also for quaternion-valued stationary signals by simply adapting the proof.

As a corollary, after developing $\mathrm{d}X(\nu)$ in (78) in terms of $\mathrm{d}U, \mathrm{d}V$ components and using (72), (73), (75) yields the general expression (20) of the autocovariance $\gamma_{xx}[\tau]$ by inverse QFT. In particular for $\tau = 0$ one obtains (15).

References

[1] J. Gonella, "A rotary-component method for analysing meteorological and oceanographic vector time series," in *Deep Sea Research and Oceanographic Abstracts*, vol. 19, no. 12. Elsevier, 1972, pp. 833–846.

[2] C. N. Mooers, "A technique for the cross spectrum analysis of pairs of complex-valued time series, with emphasis on properties of polarized components and rotational invariants," in *Deep Sea Research and Oceanographic Abstracts*, vol. 20, no. 12. Elsevier, 1973, pp. 1129–1141.

[3] B. I. Erkmen and J. H. Shapiro, "Optical coherence theory for phase-sensitive light," in *SPIE Optics+ Photonics*. International Society for Optics and Photonics, 2006, pp. 63 050G–63 050G.

[4] A. Ahrabian, N. U. Rehman, and D. Mandic, "Bivariate empirical mode decomposition for unbalanced real-world signals," *IEEE Signal Processing Letters*, vol. 20, no. 3, pp. 245–248, 2013.

[5] J. Samson, "Pure states, polarized waves, and principal components in the spectra of multiple, geophysical time-series," *Geophysical Journal International*, vol. 72, no. 3, pp. 647–664, 1983.

[6] V. Sakkalis, "Review of advanced techniques for the estimation of brain connectivity measured with eeg/meg," *Computers in biology and medicine*, vol. 41, no. 12, pp. 1110–1117, 2011.

[7] M. B. Priestley, *Spectral analysis and time series*. Academic press, 1981.

[8] P. J. Brockwell and R. A. Davis, *Time series: theory and methods*. Springer Science & Business Media, 2013.

[9] B. Picinbono and P. Bondon, "Second-order statistics of complex signals," *IEEE Transactions on Signal Processing*, vol. 45, no. 2, pp. 411–420, Feb 1997.

[10] P. Amblard, M. Gaeta, and J. Lacoume, "Statistics for complex variables and signals, part 1: Variables," *Signal Processing*, vol. 53, no. 1, pp. 1–13, 1996.

[11] ——, "Statistics for complex variables and signals, part 2: Signals," *Signal Processing*, vol. 53, no. 1, pp. 15–25, 1996.

[12] P. J. Schreier and L. L. Scharf, *Statistical signal processing of complex-valued data: the theory of improper and noncircular signals*. Cambridge University Press, 2010.

[13] T. Adali, P. J. Schreier, and L. L. Scharf, "Complex-valued signal processing: The proper way to deal with impropriety," *IEEE Transactions on Signal Processing*, vol. 59, no. 11, pp. 5101–5125, 2011.

[14] P. J. Schreier, "Polarization ellipse analysis of nonstationary random signals," *IEEE Transactions on Signal Processing*, vol. 56, no. 9, pp. 4330–4339, 2008.

[15] A. T. Walden, "Rotary components, random ellipses and polarization: a statistical perspective," *Philosophical Transactions of the Royal Society of London A: Mathematical, Physical and Engineering Sciences*, vol. 371, no. 1984, p. 20110554, 2013.
[16] A. T. Walden and T. Medkour, "Ensemble estimation of polarization ellipse parameters," *Proceedings of the Royal Society A: Mathematical, Physical and Engineering Sciences*, vol. 463, no. 2088, pp. 3375–3394, 2007. [Online]. Available: http://rspa.royalsocietypublishing.org/cgi/doi/10.1098/rspa.2007.0072
[17] P. Rubin-Delanchy and A. T. Walden, "Kinematics of complex-valued time series," *IEEE Transactions on Signal Processing*, vol. 56, no. 9, pp. 4189–4198, 2008.
[18] S. Chandna and A. T. Walden, "Statistical properties of the estimator of the rotary coefficient," *IEEE Transactions on Signal Processing*, vol. 59, no. 3, pp. 1298–1303, 2011.
[19] ——, "Simulation methodology for inference on physical parameters of complex vector-valued signals," *IEEE Transactions on Signal Processing*, vol. 61, no. 21, pp. 5260–5269, 2013.
[20] C. Brosseau, *Fundamentals of polarized light: a statistical optics approach*. Wiley-Interscience, 1998.
[21] ——, "Statistics of the normalized Stokes parameters for a Gaussian stochastic plane wave field," *Applied Optics*, vol. 34, no. 22, pp. 4788 – 4793, 1995.
[22] R. Barakat, "Statistics of the Stokes parameters," *Journal of the Optical Society of America A*, vol. 4, no. 7, pp. 1256–1263, 1987. [Online]. Available: http://josaa.osa.org/abstract.cfm?URI=josaa-4-7-1256
[23] ——, "The Statistical Properties of Partially Polarized Light," *Optica Acta: International Journal of Optics*, vol. 32, no. 3, pp. 295–312, 1985. [Online]. Available: http://www.tandfonline.com/doi/abs/10.1080/713821736
[24] D. Giuli, "Polarization Diversity in Radars," *Proceedings of the IEEE*, vol. 74, no. 2, pp. 245–269, 1986.
[25] J. Flamant, N. L. Bihan, and P. Chainais, "Time-frequency analysis of bivariate signals," *Applied and Computational Harmonic Analysis*, pp. –, 2017.
[26] J. Flamant, N. Le Bihan, and P. Chainais, "Polarization spectrogram of bivariate signals," in *IEEE International Conference on Acoustics, Speech, and Signal Processing (ICASSP), 2017, New Orleans, USA*, 2017.
[27] J. H. Conway and D. A. Smith, *On quaternions and octonions: their geometry, arithmetic, and symmetry*, 2003.
[28] T. Bulow and G. Sommer, "Hypercomplex signals-a novel extension of the analytic signal to the multidimensional case," *IEEE Transactions on Signal Processing*, vol. 49, no. 11, pp. 2844–2852, 2001.
[29] N. Le Bihan, S. J. Sangwine, and T. A. Ell, "Instantaneous frequency and amplitude of orthocomplex modulated signals based on quaternion fourier transform," *Signal Processing*, vol. 94, pp. 308–318, 2014.
[30] A. M. Yaglom, "An Introduction to the Theory of Stationary Random Functions," p. 235, 1962.
[31] A. Blanc-Lapierre and R. Fortet, *Théorie des Fonctions Aléatoires*. Paris: Masson, 1953.
[32] N. N. Vakhania, "Random vectors with values in quaternion hilbert spaces," *Theory of Probability & Its Applications*, vol. 43, no. 1, pp. 99–115, 1999.
[33] P.-O. Amblard and N. Le Bihan, "On properness of quaternion valued random variables," in *Proc. IMA Conf. Mathematics in Signal Processing*, 2004, pp. 23–26.
[34] J. Via, D. Ramirez, and I. Santamaria, "Properness and Widely Linear Processing of Quaternion Random Vectors," *IEEE Transactions on Information Theory*, vol. 56, no. 7, pp. 3502–3515, 2010.
[35] N. Le Bihan. (2016) The geometry of proper quaternion random variables. ArXiv preprint arXiv:1505.06182, November 2016.
[36] G. G. Stokes, "On the Change of Refrangibility of Light," *Philosophical Transactions of the Royal Society of London*, vol. 142, no. 1852, pp. 463–562, 1852.
[37] M. Born and E. Wolf, *Principles of optics: electromagnetic theory of propagation, interference and diffraction of light*. CUP Archive, 2000.
[38] H. Poincaré, *Théorie mathématique de la lumiere II*, 1892.
[39] N. Kikuchi, "Analysis of signal degree of polarization degradation used as control signal for optical polarization mode dispersion compensation," *Lightwave Technology, Journal of*, vol. 19, no. 4, pp. 480–486, 2001. [Online]. Available: http://ieeexplore.ieee.org/iel5/50/19910/00920845.pdf?tp={&}isnumber=19910{&}arnumber=920845{&}punumber=50
[40] R. Shirvany, M. Chabert, and J. Y. Tourneret, "Ship and oil-spill detection using the degree of polarization in linear and hybrid/compact dual-pol SAR," *IEEE Journal of Selected Topics in Applied Earth Observations and Remote Sensing*, vol. 5, no. 3, pp. 885–892, 2012.
[41] D. B. Percival and A. T. Walden, *Spectral analysis for physical applications*. Cambridge University Press, 1993.
[42] D. J. Thomson, "Spectrum estimation and harmonic analysis," *Proceedings of the IEEE*, vol. 70, no. 9, pp. 1055–1096, 1982.
[43] A. T. Walden, "A unified view of multitaper multivariate spectral estimation," *Biometrika*, vol. 87, no. 4, pp. 767–788, 2000.
[44] D. Slepian, "Prolate spheroidal wave functions, fourier analysis, and uncertaintyv: The discrete case," *Bell System Technical Journal*, vol. 57, no. 5, pp. 1371–1430, 1978.
[45] T. Medkour and A. T. Walden, "Statistical Properties of the Estimated Degree of Polarization," *IEEE Transactions on Signal Processing*, vol. 56, no. 1, pp. 408–414, 2008.
[46] V. Santalla del Rio, J. M. Pidre Mosquera, M. Vera Isasa, and M. E. de Lorenzo, "Statistics of the Degree of Polarization," *IEEE Transactions on Antennas and Propagation*, vol. 54, no. 7, pp. 2173–2175, 2006.